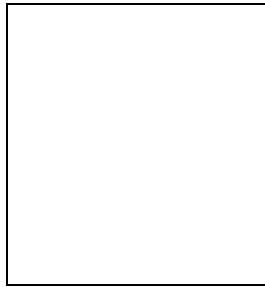


# NEUTRINO ASTRONOMY AT THE SOUTH POLE

P.A. TOALE<sup>a</sup>

*The Pennsylvania State University  
Department of Physics  
104 Davey Lab, PMB046  
University Park, PA, 16802*



IceCube is currently being built deep in the glacial ice beneath the South Pole. In its second year of construction, it is already larger than its predecessor, AMANDA. AMANDA continues to collect high energy neutrino and muon data as an independent detector until it is integrated with IceCube. After introducing both detectors, recent results from AMANDA and a status report on IceCube are presented.

## 1 Introduction

Traditional astronomical observations utilize photons or charged particles. Photons are detected over a wide range of energies, from the 2.7 K cosmic microwave background up to 10 TeV gamma rays. Unfortunately photon astronomy is not possible at higher energies due to interactions with interstellar gases and radiation fields. Cosmic rays are detected at even higher energies, and the energy spectrum has been measured out as high as  $10^{11}$  GeV. However, all but the highest energy rays (above  $10^{10}$  GeV) are bent in the galactic magnetic field, obscuring the identity of their sources.

There are a variety of models that account for the high energy photons and charged particles that are observed. These can be divided into two categories: hadronic acceleration and exotic particle decay. The first category contains the so-called bottom-up models since they all involve acceleration of hadrons, typically protons, to very high energy. Candidates for these cosmic accelerators include Active Galactic Nuclei, Supernova remnants, and Gamma Ray Bursts. Models of the second category are known as top-down since they contain a heavy exotic particle

---

<sup>a</sup>On behalf of the IceCube Collaboration, see <http://icecube.wisc.edu/science/publications/moriond2006.html>.

decaying into energetic Standard Model particles. Examples include topological defects such as magnetic monopoles and generic Weakly Interacting Massive Particles (WIMPs).

Most of these models predict neutrino production in addition to photons and cosmic rays. The goal of neutrino astronomy is to discover and measure these high energy neutrinos. Neutrinos offer several advantages over traditional astronomical messengers. First, they are weakly interacting, so they can travel cosmological distances without being scattered or absorbed. Second, they are electrically neutral, so they are not deflected by interstellar magnetic fields. Together, these two qualities make neutrinos excellent discovery instruments.

The same properties that make neutrinos good astronomical messengers also make them difficult to detect. The most successful technique for observing extraterrestrial neutrinos works by detecting Cherenkov light produced by secondary particles arising from neutrino interactions. The signature of light differs depending on the flavor of the neutrino and the type of interaction. For instance, muon neutrinos can interact via a charged current (CC) interaction and produce a long lived muon with a conical light pattern, whereas CC interactions of electron neutrinos produce electromagnetic showers with a more spherical pattern. Tau neutrinos produce tau leptons in CC interactions which, depending on the size of the detector, may decay back into tau neutrinos plus other particles, resulting in a combination of track-like and shower-like patterns. The neutral current (NC) interaction of all three flavors result in hadronic showers, which are probably not distinguishable from electromagnetic showers.

In order to detect the fluxes predicted by accepted cosmological models, one needs either to wait a very long time or to build a very big detector. This leads to the search for naturally occurring, optically transparent media. Several groups have implemented the optical Cherenkov technique in large volumes of water or ice. The two media differ both in optical properties and in inherent backgrounds. Water typically has a long scattering length ( $> 100$  m) but a short absorption length ( $\sim 20$  m). Deep ice<sup>1</sup> on the other hand, has a long absorption length ( $\sim 110$  m) but a short scattering length ( $\sim 20$  m). Also, ice is nearly free of light-producing backgrounds while water contains biological and chemical sources such as potassium decay in salt water. The rest of this paper focuses on neutrino detection in deep ice as pioneered by the Antarctic Muon and Neutrino Detector Array (AMANDA) and carried on today by IceCube.

## 2 AMANDA

AMANDA has applied the optical Cherenkov technique using deep, clear ice below the Amundsen–Scott South Pole station. The current detector consists of 19 instrumented strings, deployed between 1500 – 2000 m below the ice surface. Each string contains between 20 to 42 optical modules (OMs), spaced vertically by 10 – 20 m. There are a total of 677 OMs in the ice, each of which is composed of an 8-inch photomultiplier tube (PMT) housed in a glass pressure sphere. The PMT signals are sent to the surface over either twisted pair, coaxial, or fiber optic cable where they are processed by the surface data acquisition system. The instrumented region of AMANDA is cylindrical in shape with a 200 m diameter and a height of 500 m.

The AMANDA detector is best suited for detection of muons. These can be atmospheric muons produced from cosmic rays or muons produced from muon neutrino interactions. These muon neutrinos can arise from cosmic rays interaction with the atmosphere or from the much anticipated cosmological progenitors. High energy muons travel long distances through the ice, *e.g.* a 200 GeV muon can travel up to 1 km. At the depth of AMANDA (and IceCube), the rate of down-going atmospheric muons is a million times higher than the rate of muons from atmospheric neutrinos. Therefore the characteristic signature of muon neutrinos in AMANDA is muon tracks traveling upwards through the detector toward the surface.

The direction (space-angle) of muon tracks passing through the detector can be reconstructed with an accuracy of  $2 - 3^\circ$ . Since the direction of the primary muon neutrino differs

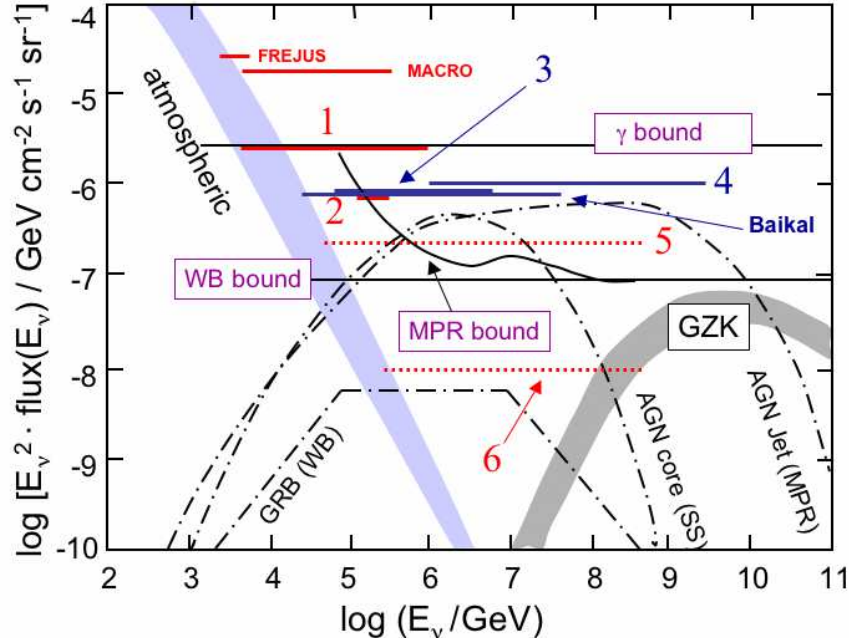


Figure 1: Diffuse neutrino flux limits shown with expected atmospheric contribution and several leading cosmological models. The limits are calculated assuming oscillations with full mixing, so the  $\nu_\mu$  limits are shown multiplied by 3.

from the direction of the muon by  $\sim 1^\circ$  at 1 TeV, the neutrino points back toward its source with similar accuracy. The energy reconstruction is much less precise because it is based on radiative losses of the muon as it passes through the detector. Fluctuations in these losses result in an energy resolution of 30% in the logarithm of energy.

Cascade reconstruction is significantly different. Light from cascades is produced over  $\sim 10$  m which, given the spacing of the OMs, results in a degraded angular resolution of  $30 - 40^\circ$ . On the other hand, cascades are likely to be contained within the detector, giving them a better energy resolution (as good as 10% in  $\log E$ ).

### 2.1 A Selection of AMANDA Results

AMANDA analyses fall into three broad categories: measurement of the energy spectrum of the diffuse neutrino flux, searches for neutrino point sources, and search for new physics in the form of exotic particles or violation of conservation laws. A summary of each of the categories is given below.

The diffuse flux is studied by first measuring the energy spectrum of up-going muons and then unfolding resolution effects to arrive at the neutrino energy spectrum. The spectrum has been measured from 1 – 100 TeV and agrees well with both atmospheric models and lower energy data from the Frejus experiment<sup>2</sup>. Preliminary results from the AMANDA data give a spectral index of  $3.54 \pm 0.11$ <sup>3</sup>. There is no indication of excess events above the expected atmospheric contribution in this energy range.

Figure 1 shows upper limits and sensitivities from several independent analyses, along with predictions from several leading models. Limits (1), (3), and (4) are published results from three independent AMANDA analyses<sup>4,5,6</sup>. Limit (2), along with sensitivities (5) and (6), are preliminary AMANDA results<sup>7,8,9</sup>. Also shown are limits from Frejus<sup>2</sup>, MACRO<sup>10</sup>, and Baikal<sup>11</sup>.

The point-source analysis uses 3329 up-going events collected from 2000 to 2003<sup>12</sup>. The

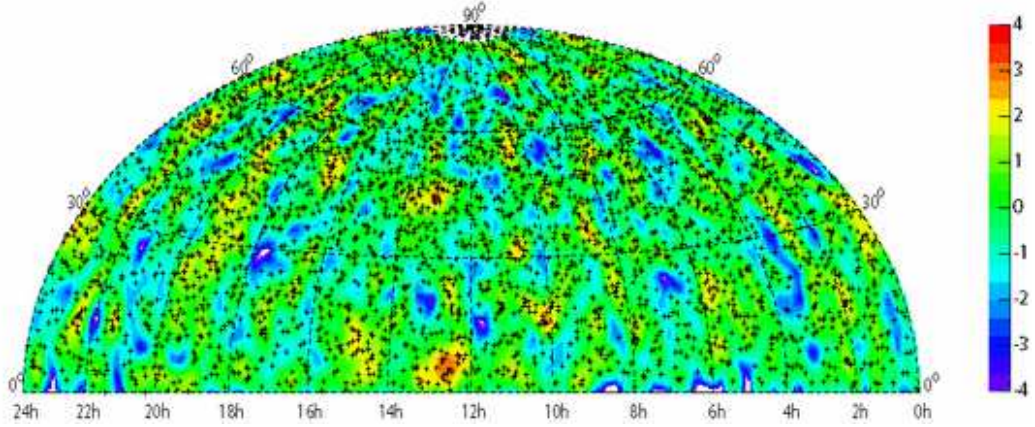


Figure 2: Northern hemisphere of the neutrino sky map based on 3329 muon neutrino events. Colors indicate Gaussian standard deviations from the expected isotropic distribution.

resulting, preliminary, sky map, shown in Figure 2, is consistent with isotropic atmospheric neutrinos. The maximum observed deviation is  $3.4\sigma$ , which has a chance occurrence of 92%. A catalog of 33 known astronomical sources is also studied, of which the most significant excess is observed from the Crab nebula with 10 events and an expected background of 5.4. The chance probability of this excess is 64%.

AMANDA continues to search for dark matter in the form of neutralinos. In many models the neutralino is the lightest supersymmetric particle and is stable if R-parity is conserved. Over time, these particles will accumulate at the bottom of gravitational wells, such as the center of the sun. The rate at which they collect depends on several factors, such as their density and velocity distributions, their cross sections for interacting with ordinary matter, and their annihilation cross section. The annihilation products include  $q\bar{q}$ ,  $l\bar{l}$ , as well as  $W^\pm$ ,  $Z$ , and  $H$ , with  $b\bar{b}$ ,  $\tau^+\tau^-$ , and  $W^+W^-$  dominating. Many of the secondary decays include neutrinos.

The analysis is therefore optimized to detect neutrinos produced in the sun or in the center of the earth. So far, only the muon neutrino channel has been probed. No excess has been observed from either source. Figure 3 shows exclusion plots of muon flux as a function of neutralino mass. In both, the hashed region shows the sensitivity of the CDMS experiment, with the green area excluded at the one sigma level. The plot on the left shows the upper limit from the center-of-earth analysis<sup>13</sup>, while the one on the right shows the results from the center-of-sun analysis<sup>14</sup>.

### 3 IceCube

IceCube differs from AMANDA in two important ways. First, IceCube will be much larger, with a final fiducial volume of approximately one cubic kilometer. Second, PMT signals are digitized in situ by electronics housed in the optical module.

IceCube will eventually consist of 70 or more strings with 60 modules each. The modules are spaced by 17 m vertically while the strings are arranged in a hexagonal pattern with a spacing of 125 m. In addition to the in-ice array, there is a surface cosmic ray detector named IceTop. At the position of each in-ice string there is a surface station comprised of two tanks, each containing two DOMs frozen in clear ice.

The heart of IceCube is the Digital Optical Module (DOM) that consists of a 10 in. PMT together with fast digitization electronics. Signals are processed by both an Advanced Transient Waveform Digitizer (ATWD) and a long running Fast Analog-to-Digital Converter (FADC). The ATWD contains three channels with different gains and has a programmable sampling rate

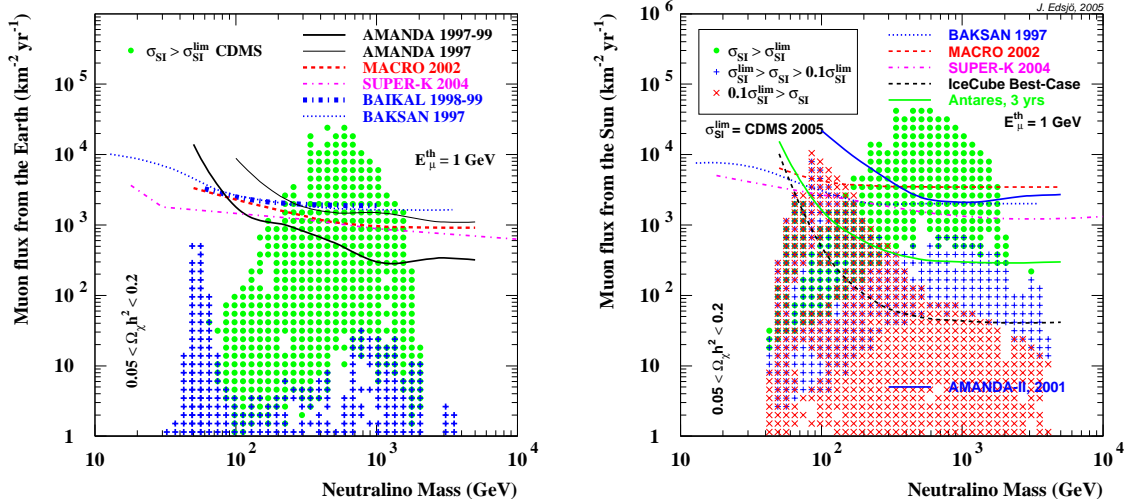


Figure 3: Upper limits on mass dependent muon neutrino fluxes from the center of the earth (left) and the center of the sun (right). In both cases the CDMS results are shown as the hashed region with the green area laying within  $1 \sigma$  of their spin-independent limit.

from 200 – 700 MHz for a maximum range of 400 ns. The FADC, on the other hand, samples at a fixed rate of 40 MHz but has a range of  $6.4 \mu\text{s}$ .

The dark noise rates of the DOM in ice is 650 Hz. This rate is reduced in the ice by local coincidence logic which makes use of information from neighboring DOMs. By requiring activity in a neighbor in a 800 ns time window, the rate is reduced to 15 Hz on average.

Construction of IceCube began in the Austral summer of 2004-2005 with the deployment of a single in-ice string and four surface stations and continued in 2005-2006 with eight strings and 12 stations. Construction is scheduled to continue through 2010.

### 3.1 IceCube First Year Performance

IceCube collected data with its first string (String 21) of modules throughout 2005. Studies of initial performance<sup>15</sup> indicate that the design goals have been met.

In particular, the average dark-noise rate, with a  $51 \mu\text{s}$  deadtime to suppress afterpulses, on String 21 is less than 400 Hz per DOM, with somewhat higher rates in the deepest modules. The time calibration system has been verified and shown to have an intrinsic resolution of less than 3 ns. The overall timing resolution has been studied with light sources on the DOM and seen to be as good as 3 ns.

Muon tracks have also been reconstructed. The hit multiplicity and zenith angle distributions match expectations from simulated atmospheric muons. The space-angle resolution, with one string, is found to vary from  $9.7^\circ$ , for low multiplicity events, to  $1.5^\circ$ , for high multiplicity events.

Finally, a search for upward-going events resulted in two candidate events in six months of data. The events had multiplicities of 35 and 50 (out of 60) and zenith angles of  $178.8^\circ$  and  $179.1^\circ$ , respectively (errors are statistical only). Two events in this time period is consistent with predictions from simulation<sup>16</sup>.

The verification of the 9-string, 16-station array is now underway. More than 99% of the modules are operational and preliminary analysis indicates that the detector is functioning as designed.

## 4 Conclusion

The AMANDA detector continues the exploration of the high energy neutrino sky and will soon be an integral part of its successor, IceCube. IceCube has deployed 9 in-ice strings and 16 surface stations and early results are promising.

## Acknowledgments

In addition to acknowledging the sources listed at the URL given in footnote (a), the author wishes to acknowledge NSF award number PHY-0611671 and EU contract number MSCF-CT-2004-516636 for support in attending this conference.

## References

1. M. Ackermann *et al.* (AMANDA Collaboration), *J. Geophys. Res.*, In Press, doi:10.1029/2005JD006687.
2. K. Daum *et al.*, *Z. Phys. C* **266**, 417 (1995).
3. H. Geenen, *Energy reconstruction and spectral unfolding of atmospheric leptons with the AMANDA detector*, thesis Universität Wuppertal, 2002.
4. J. Ahrens *et al.*, *Astropart. Phys.* **90**, 251101 (2003).
5. M. Ackermann *et al.*, *Astropart. Phys.* **22**, 127 (2004).
6. M. Ackermann *et al.*, *Astropart. Phys.* **22**, 339 (2005).
7. K. Münich for the IceCube collaboration, ICRC Pune 2005.
8. L. Gerhardt for the IceCube collaboration, ICRC Pune 2005.
9. L. Hodges for the IceCube collaboration, ICRC Pune 2005.
10. M. Ambrosio *et al.*, *Astropart. Phys.* **19**, 1 (2003).
11. V. Aynutdinov *et al.*, *Astropart. Phys.* **25**, 140 (2006).
12. A. Achterberg *et al.* (IceCube Collaboration), astro-ph/0509330.
13. A. Achterberg *et al.*, accepted for publication in *Astropart. Phys.*.
14. A. Achterberg *et al.*, *Astropart. Phys.* **24**, 459 (2006).
15. A. Achterberg *et al.* (IceCube Collaboration), astro-ph/0604450.
16. J. Ahrens *et al.* (IceCube Collaboration), *Astropart. Phys.* **20**, 507 (2004).